analytical chemistry

pubs.acs.org/ac Article

A Flexible Microfluidic Chip-Based Universal Fully Integrated Nanoelectronic System with Point-of-Care Raw Sweat, Tears, or Saliva Glucose Monitoring for Potential Noninvasive Glucose Management

Mimi Sun, Xinyi Pei, Tong Xin, Jian Liu, Chongbo Ma, Mengzhu Cao, and Ming Zhou*

Cite This: *Anal. Chem.* 2022, 94, 1890−1900 Read Online

ACCESS | Metrics & More | Article Recommendations | Supporting Information

ABSTRACT: By combining the distinctive noninvasive feature with the peculiar complete functional implementation trait, fully integrated raw noninvasive biofluid glucose biosensors offer active and remote glucose monitoring while posing minimal harm or infection risks compared to the traditional invasive manner. However, each previously reported fully integrated raw noninvasive biofluid glucose biosensor is solely focused on single-type raw noninvasive biofluid analysis. Given the diversity and complexity of subjects' physical conditions, single-type raw noninvasive biofluids are inappropriate to all crowds (e.g., sweat collection/analysis could be inapplicable for dermatopathic subjects). Here, we demonstrate the first example of a universal fully integrated nanoelectronic system with the unique capability to point-of-care and universally monitor diverse raw noninvasive biofluid (i.e., sweat, tears, and saliva) glucose by combining a flexible and disposable microfluidic enzymatic biosensor (named *iez*Slice) for raw biofluid pump-free sampling and measurement with a customized, handheld, and reusable wireless electronic device (named *iez*Bar) for electrical signal transduction, conditioning, processing, and wireless transmission. We employed the specially designed high-concentration-buffer powder-loaded Kimwipes (HBP-KWs) as the microfluidic channel (microchannel) of *iez*Slice, guaranteeing a high-accuracy glucose analysis in various raw noninvasive biofluids. We also evaluated the potential utility of the universal fully integrated nanoelectronic system for noninvasive glucose management in healthy and diabetic subjects with the assistance of the proposed volatility-derived blood glucose concentration-free protocol. Although we focus on raw noninvasive biofluid glucose analysis in this work, the universal fully integrated nanoelectronic system may readily realize accurate monitoring of various biomolecules in raw noninvasive biofluids by introducing corresponding bioreceptors.

INTRODUCTION

Intertwined with concepts of noninvasive biofluid analysis and portable diagnosis, the point-of-care noninvasive biofluid monitoring with the direct utilization of raw noninvasive biofluids as the sample media offers the features to expediently seek precautions and medical attention as well as to timely track the cognitive status concerning therapy,[1−4] which provides a meritorious insight toward personalized healthcare and health management.[5−8] Compared to the traditional biomedical "gold standard" biospecimens of invasive biofluids that have to be collected via the invasive puncture,[9] the noninvasive biofluids with the minimal risk of harm or infection risks for sampling also contain important and rich electrolytes, hormones, metabolites, proteins, and amino acids, which allows for the monitoring of metabolic diseases, physiological conditions, or an individual's level of intoxication.[1,10] For example, sweat chloride and saliva human immunodeficiency virus (HIV) antibodies are proved to be the biomarkers of cystic fibrosis[11] and acquired immune deficiency syndrome (AIDS),[12] respectively, and the usefulness of tears in therapeutical monitoring of acetaminophen drug has been successfully demonstrated.[13]

Fully integrated devices that enable fully functional operation but do not require external accessories are considered to be one of the most desirable and ultimate objectives for advanced device design and engineering.[14] By introducing the fully integrated concept into the raw noninvasive biofluid analysis field, the fully integrated raw noninvasive biofluid biosensors demonstrate the potential to

Received: November 29, 2021
Accepted: January 3, 2022
Published: January 10, 2022

https://doi.org/10.1021/acs.analchem.1c05174
Anal. Chem. 2022, 94, 1890−1900

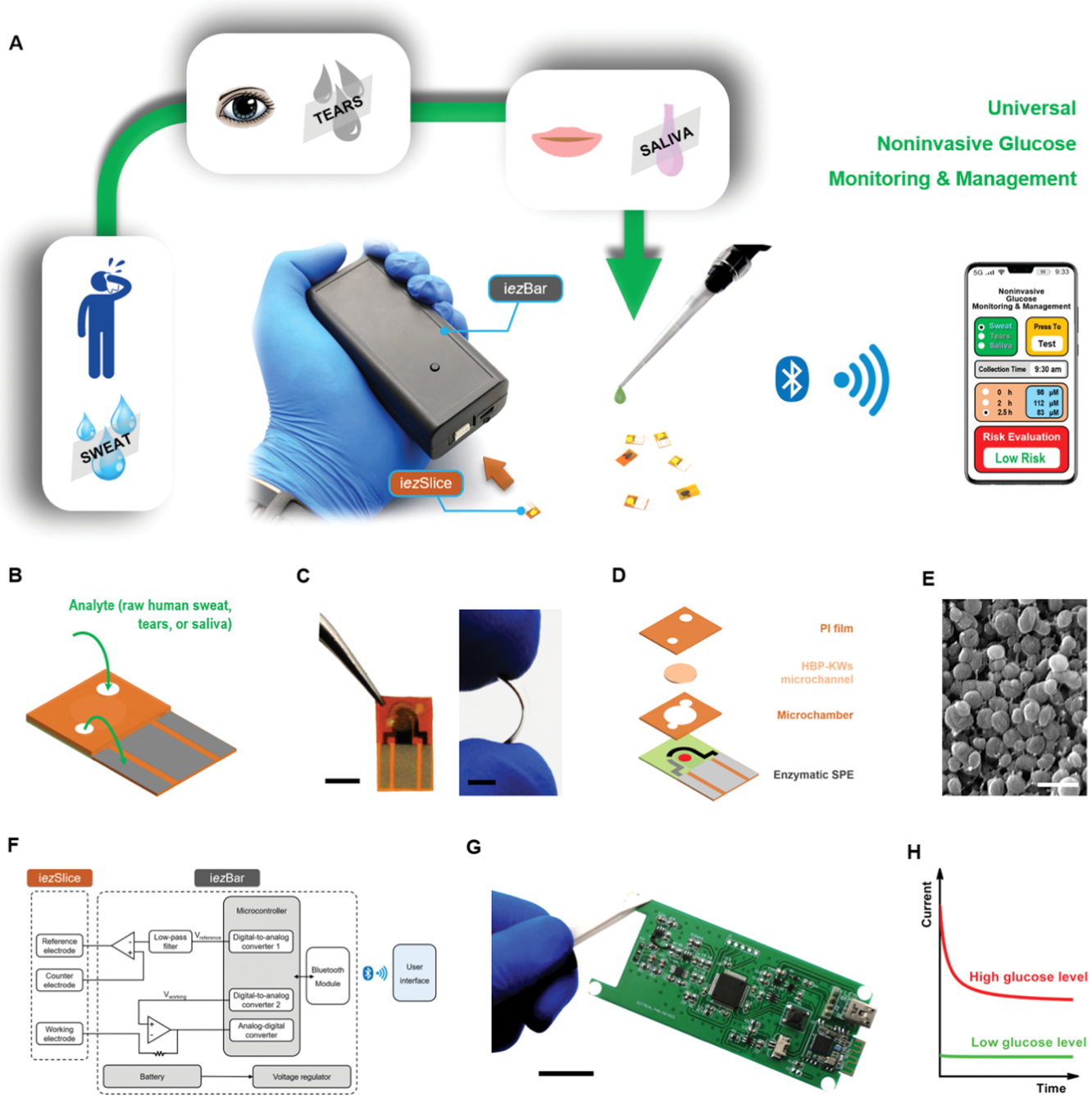

Figure 1. Schematics of a universal fully integrated nanoelectronic system with point-of-care glucose monitoring from a single drop of raw human sweat, tears, or saliva for potential noninvasive glucose management. (A) Illustration of a universal fully integrated nanoelectronic system that incorporates an *iez*Slice (i.e., a microfluidic enzymatic biosensor) and an *iez*Bar (i.e., a customized wireless potentiostat). (B) Schematic of an *iez*Slice. (C) Photographic images of the *iez*Slice in flat (left) and bent states (right). Scale bars, 3 mm (left) and 1.5 mm (right). (D) Schematic representation of the components of an *iez*Slice. (E) SEM image of the 3D-CNAs. Scale bar, 300 nm. (F) System-level block diagram illustrating the signal transduction, conditioning, processing, and wireless transmission from *iez*Slice to *iez*Bar and the user interface. (G) Photographic image of the customized circuit board of an *iez*Bar. Scale bar, 2 cm. (H) Detection of raw sweat, tears, or saliva glucose with amperometry by which the glucose level is determined from the current.

supplement laboratory-based invasive tests in allowing convenient daily health status monitoring as well as early illness detection and management.[15] As a serious, long-term, chronic hyperglycemic but easily neglected disease, diabetes mellitus always requires frequently adjusted external insulin dose treatment depending on the individual's pancreatic β-cell activities and daily glucose uptake.[16] Such a scenario necessitates the frequent glucose monitoring on both healthy and diabetic subjects for preventive and therapeutic glucose management,[17] respectively, which drives the raw invasive biofluid (e.g., blood) glucose meter to be one of the most popular and successful fully integrated devices in the world.[9,18,19]

Recent advances in fully integrated raw noninvasive biofluid biosensors have opened up a window of opportunities for hassle-free and personalized noninvasive glucose monitoring

https://doi.org/10.1021/acs.analchem.1c05174
Anal. Chem. 2022, 94, 1890−1900

and management.[1,3,15,20] For example, prolific research studies toward the development of fully integrated raw sweat glucose biosensors greatly expand the horizons of personalized noninvasive glucose management.[11,14,21−29] In another case, Wang's group from the University of California San Diego pioneered an eyeglasses-based fully integrated glucose biosensor that focuses on the analysis of raw tears and paves the way for the widespread application of the fully integrated raw tears glucose biosensors.[30] Lately, Mitsubayashi's group from Tokyo Medical and Dental University developed a fully integrated glucose biosensor that is built in a mouthguard and committed to raw saliva glucose monitoring for the noninvasive management of diabetes patients.[31] To date, each reported fully integrated raw noninvasive biofluid glucose biosensor generally focused on single-type noninvasive biofluid analysis, which invalidates these devices for noninvasive glucose measurement under the circumstances that such one specific type of biofluid is unable to collect and accordingly tremendously limits their practicability. To the best of our knowledge, the universal point-of-care glucose analysis in diverse-type raw noninvasive biofluids by a single fully integrated raw noninvasive biofluid glucose biosensor has not been reported and realized.

Here, we present the first development of a fully integrated point-of-care noninvasive biofluid nanoelectronic device that is able to universally and accurately analyze glucose in all three of the most common-type noninvasive biofluids of sweat, tears, and saliva for potential noninvasive glucose management using an easy-to-use, handheld, simple, portable, pump-free, and wireless universal fully integrated nanoelectronic system on the basis of a flexible microfluidic chip (microchip). The employment of the high-concentration-buffer powder-loaded Kimwipes (HBP-KWs) as the pump-free microfluidic channel (microchannel) enables the distinctive feature of universal glucose analysis in raw noninvasive biofluids of sweat, tears, and saliva with high accuracy. The application of the nanoscaled carbon of three-dimensional carbonaceous nanosphere network aerogels with hierarchical architectures (3D-CNAs) as the electrode material achieves a wide linear range for glucose measurement that covers the physiological glucose level ranges of the raw noninvasive biofluids of sweat, tears, and saliva. The ultralow volume of 0.30 μL for noninvasive biofluid glucose monitoring may promise quick biofluid acquisition that could most likely prompt the noninvasive biofluid glucose analysis with high time resolution and timely noninvasive glucose management. The full integration-oriented idea for the point-of-care nanoelectronic system design and construction ensures the complete functional implementation of pump-free sampling, accurate measurement, and wireless monitoring on a single-drop noninvasive biofluid of raw sweat, tears, or saliva within one solo palm-sized nanoelectronic device, which facilitates noninvasive glucose monitoring. Noninvasive glucose management, which is primarily realized on both typical healthy and diabetic subjects by the universal fully integrated nanoelectronic, illustrates an attractive and convenient way to monitor blood glucose status while posing minimal harm or infection risks. By replacing the glucose oxidase (GOx) with other biomimetic receptors, a wide range of targets could be also monitored in raw noninvasive biofluids, suggesting the high versatility of the universal fully integrated nanoelectronic system. The combination of these distinctive features with an ultralow feedstock cost of ∼USD 0.02 per test allows such a universal fully integrated nanoelectronic system to be at par or transcend the benefits and utility of conventional noninvasive biofluid glucose analysis, with bright prospects in potential point-of-care noninvasive glucose management for large-scale personal/clinical screening.

EXPERIMENTAL SECTION

Materials and Reagents. Glucose, ascorbic acid, dopamine, epinephrine, uric acid, acetaminophen, chitosan, nitric acid, lactate, fructose, maltose, sodium chloride (NaCl), potassium chloride (KCl), and calcium chloride ($CaCl_2$) were purchased from Shanghai Aladdin Biochemical Technology Co., Ltd. (China). Full details are listed in the Supporting Information.

Characterization and Measurements. Scanning electron microscopy (SEM) images were recorded using an XL-30 scanning electron microscope (Philips, the Netherlands). Transmission electron microscopy (TEM) images were observed using a JEM-2100 PLUS transmission electron microscope (JEOL Ltd., Japan). The total pore volume, pore size distribution, and Brunauer−Emmett−Teller (BET) surface area were measured using a Micromeritics ASAP 2020 automated analyzer (Micromeritics Instrument Corp.) at 77 K by the BET nitrogen adsorption/desorption technique. The Raman spectra were obtained using an HR800 Raman spectrometer system (Jobin Yvon, France). X-ray photoelectron spectra (XPS) were recorded on an ESCALAB 250 spectrometer (Thermo Fisher Scientific). Full details are listed in the Supporting Information.

Construction of the *iez*Slice. Full details are listed in the Supporting Information.

RESULTS AND DISCUSSION

Design of the Universal Fully Integrated Nanoelectronic System. Figure 1A illustrates the scheme of a universal fully integrated nanoelectronic system with point-of-care raw sweat, tears, or saliva glucose monitoring for noninvasive glucose management. Such a nanoelectronic system is composed of a flexible, pump-free, and disposable microfluidic enzymatic biosensor (named *iez*Slice, Figure 1B−E) with an ultralow feedstock cost of ∼USD 0.02 per each (Tables S1−S10) for the raw noninvasive biofluid sampling and glucose analysis and a customized, handheld, and reusable wireless electronic device (named *iez*Bar, Figure 1F−H) for signal transduction, conditioning, processing, and wireless transmission. The flexible *iez*Slice is composed of four components including an enzymatic screen-printed electrode (SPE) on a polyimide (PI) film, a microfluidic chamber (microchamber) patterned on a PI film with double-sided tape, a single piece of high-concentration-buffer powder-loaded Kimwipes (HBP-KWs) as the pump-free microfluidic channel (microchannel), and a PI film with patterned inlet and outlet (Figures 1D and S1−S5 and Tables S1−S10). The enzymatic SPE with a standard three-electrode configuration consists of a glucose oxidase (GOx) working electrode that utilizes the distinctive three-dimensional carbonaceous nanosphere network aerogels with hierarchical architectures (3D-CNAs) as the electrode substrate, an Ag/AgCl reference electrode, and a carbon counter electrode (Figure 1D,E). When a raw noninvasive biofluid flows into the *iez*Slice, the biofluid spontaneously transports along the HBP-KWs microchannel that forces the biofluid to possess constant/same pH and high ionic strength. The flexible and disposable *iez*Slice is connected

https://doi.org/10.1021/acs.analchem.1c05174
Anal. Chem. 2022, 94, 1890−1900

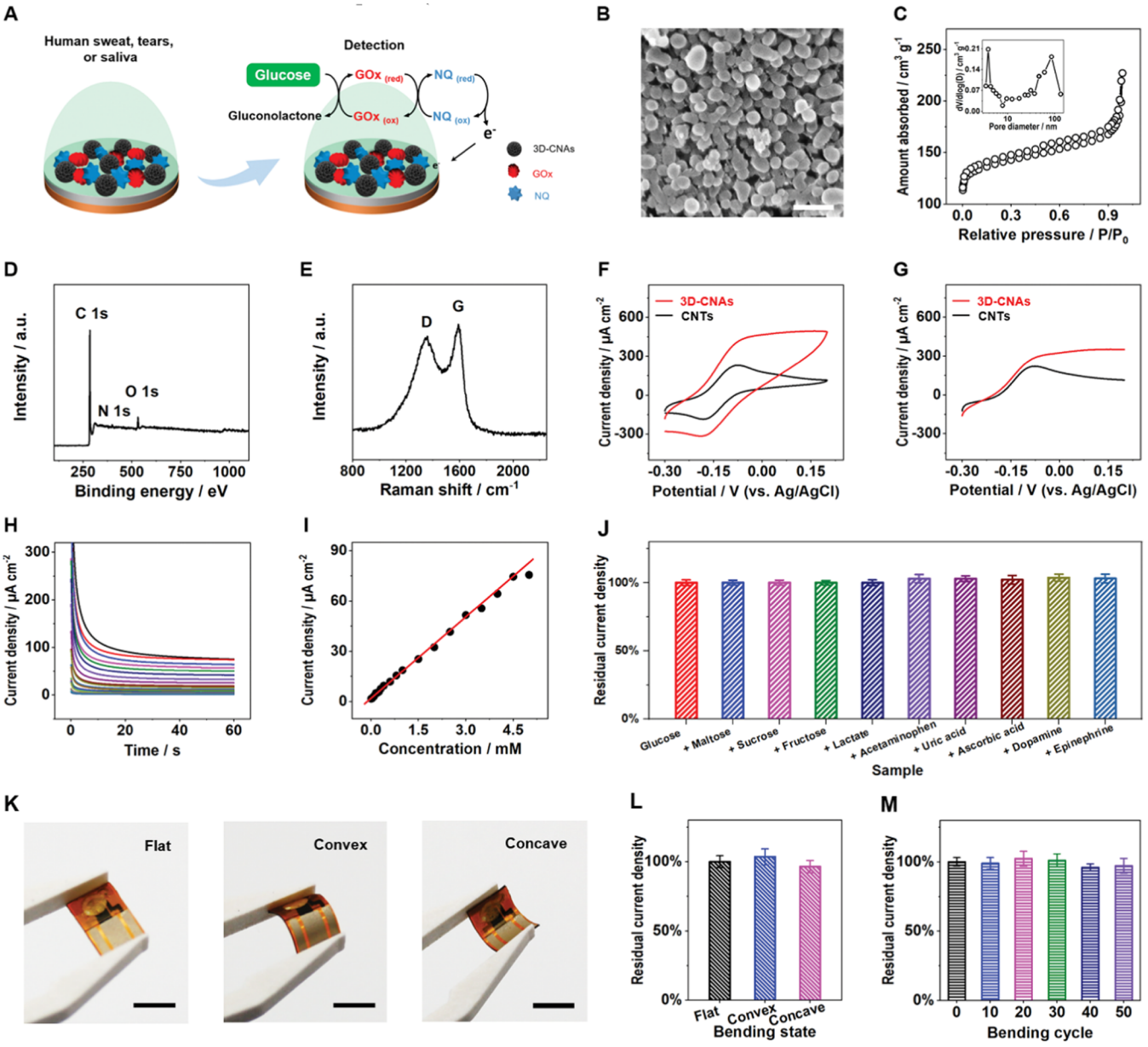

Figure 2. Schematics and characterization of the flexible *iez*Slice. (A) Schematic of an *iez*Slice that is based on a GOx-based electrochemical enzymatic biosensor for the direct raw human noninvasive biofluid glucose measurement. (B) SEM image of 3D-CNAs. Scale bar, 600 nm. (C) N_2 adsorption−desorption isotherms of 3D-CNAs. The inset shows the pore size distributions of 3D-CNAs. (D) XPS spectrum of 3D-CNAs. (E) Raman spectrum of 3D-CNAs. (F) Cyclic voltammetry (CV) curves at 3D-CNA- and CNT-based *iez*Slices for 40 mM glucose. (G) Polarization curves at 3D-CNA- and CNT-based *iez*Slices for 40 mM glucose. (H) Glucose detection with the *iez*Slice and (I) the corresponding calibration plot. (J) Selectivity of the *iez*Slice to glucose over other analytes commonly coexisting in human biofluids. The initial concentration of glucose is 1 mM, and the concentrations of other analytes are 1 mM maltose, 1 mM sucrose, 1 mM fructose, 1.5 mM lactate, 50 μM acetaminophen, 1.5 mM uric acid, 60 μM ascorbic acid, 0.5 μM dopamine, and 60 nM epinephrine. Error bars represent the standard deviations of three independent measurements. (K) Photographic images of the flexible *iez*Slice at different bending states: flat, convex, and concave states. Scale bar, 4 mm. (L) Bending state and (M) bending cycle effects on the response of the flexible *iez*Slice. Sample in (L and M), 1 mM glucose. Error bars represent the standard deviations of three independent *iez*Slices.

to a reusable *iez*Bar (Figure 1A). Figure 1F illustrates the system-level survey of such a universal fully integrated nanoelectronic system, and amperometry that is preprogrammed into the *iez*Bar is chosen to monitor the raw noninvasive biofluid glucose level based on the anodic current to facilitate further analysis and noninvasive glucose management (Figure 1H).

Design and Characterization of the *iez*Slice. The electrochemical detection of raw noninvasive biofluid (sweat, tears, or saliva) glucose at the *iez*Slice that was designed on a flexible electrochemical patch was based on a GOx-based electrochemical enzymatic biosensor (Figure 2A). To prepare the enzymatic biosensor, we sequentially modified the multilayers of 3D-CNAs, GOx, 1,4-naphthoquinone (NQ), and chitosan on one SPE as the working electrode so that the natural catalyst GOx specifically and effectively oxidizes glucose to gluconolactone with the aid of the redox mediator of NQ. Meanwhile, a Ag/AgCl electrode and a carbon

https://doi.org/10.1021/acs.analchem.1c05174
Anal. Chem. 2022, 94, 1890−1900

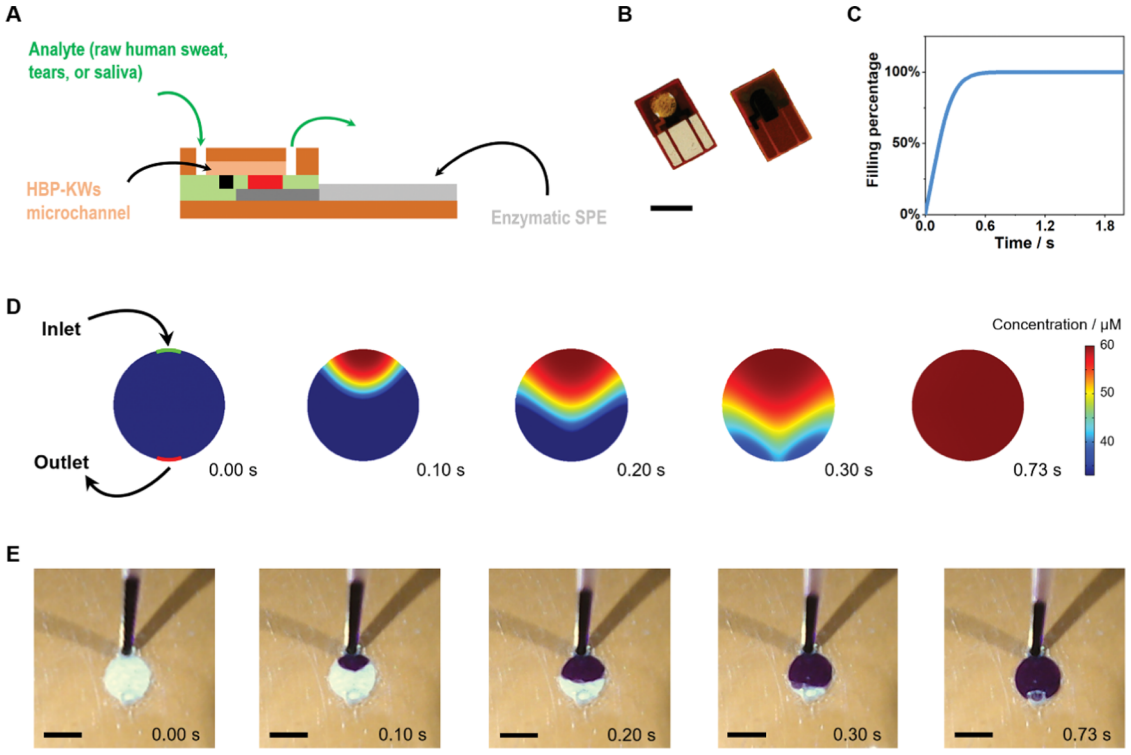

Figure 3. Design and characterization of the HBP-KWs microchannel. (A) Schematic of the sideward profile of an *iez*Slice. (B) Photographic image of the front and back sides of the *iez*Slice. Scale bar, 4 mm. (C) Simulation of the time evolution of the average sweat concentration. (D) Simulation of the distribution of sweat concentration in the microchamber under different time conditions. Green and red solid lines at 0.00 s represent the boundaries of the inlet and outlet for the simulations, respectively. (E) Photographic images of the microfluidic sweat sampling. Methyl violet dye powder was added into the sweat to make the sweat containing 20 mM methyl violet before the sampling. Scale bar, 2 mm.

electrode serve as the reference and counter electrodes, respectively.

In light of their outstanding pore accessibility and very fast mass transport, three-dimensional carbonaceous nanoscale networks are the most suitable electrode material candidate for constructing electronic devices.[32,33] To achieve the high-performance glucose determination in different types of raw noninvasive raw biofluids, the three-dimensional carbonaceous nanoscale networks of 3D-CNAs were synthesized and chosen as the electrode material of the enzymatic biosensor owing to their unique nanostructure-driven superior electrochemical capability. The 3D-CNA layer on the enzymatic biosensor surface exhibits a nanosphere network architecture (Figures 2B, S6, and S7) with a high specific surface area of 542.78 $m^2 g^{-1}$, a large pore volume of 0.14 $cm^3 g^{-1}$, and hierarchical meso-macropores (centered at 3.82, 46.40, 60.58, and 85.68 nm; Figure 2C). Such a nanoscale architecture may not only supply efficacious building blocks to achieve a high mass and compact enzyme loading but also grant continual and unhindered pathways for species permeability and conveyance, which are favorable for improving the electron transfer. The X-ray photoelectron spectroscopy (XPS) spectrum implies the existence of the N element in 3D-CNAs (Figure 2D), which is very beneficial to promote the electrocatalytic ability. The high I_D/I_G value (2.35) in the Raman spectrum signifies that there are high-density defective sites existing in 3D-CNAs (Figure 2E), which are propitious to accelerate the electron transfer.[34,35] Considering the preceding discussion, it is pretty reasonable to believe that the distinctive nanoscale network architecture of 3D-CNAs makes it extremely appealing as the electrode substrate for the enzymatic biosensor construction. By introducing 3D-CNAs into the enzymatic biosensor, the 3D-CNA-based *iez*Slice exhibits a high-performance electrocatalytic capacity for glucose that is revealed by a much higher current density but a lower onset potential compared to the one that is based on the most popular carbonaceous nanomaterial of carbon nanotubes (CNTs; Figures 2F,G and S8), implying high feasibility to utilize 3D-CNAs as an advanced electrode material of an enzymatic biosensor for the direct raw noninvasive biofluid glucose measurement with superior performance.

To explore the detection capability, the *iez*Slice was investigated by analyzing different concentrations of glucose standards. The *iez*Slice exhibits a wide linear range of 5 μM to 4.50 mM between the amperometric response and the glucose content and a low detection limit down to 0.48 μM at a signal-to-noise ratio of 3 (Figure 2H,I), which fully cover the physiological glucose level range of the raw human noninvasive biofluids of sweat, tears, and saliva.[9,36] It is worth noting that the analytical performance of such *iez*Slice with 3D-CNAs as the electrode material is not only higher than that of the *iez*Slice with CNTs as the electrode material (Figure S9 and Table S11) but also among the best ones of the reported point-of-care fully integrated biosensors for raw noninvasive biofluid glucose measurement of raw human sweat, tears, or saliva (Table S11), indicating an essential role of the 3D-CNAs. The *iez*Slice also exhibits satisfied selectivity over other analytes in raw sweat, tears, or saliva at physiologically relevant concentrations (Figure 2J), which is one of the most important prerequisites that ensure accurate glucose detection.

As an electrochemical electronic device, its signals often shift with pH[37,38] and ionic strength variations.[39,40] However, not

https://doi.org/10.1021/acs.analchem.1c05174
Anal. Chem. 2022, 94, 1890−1900

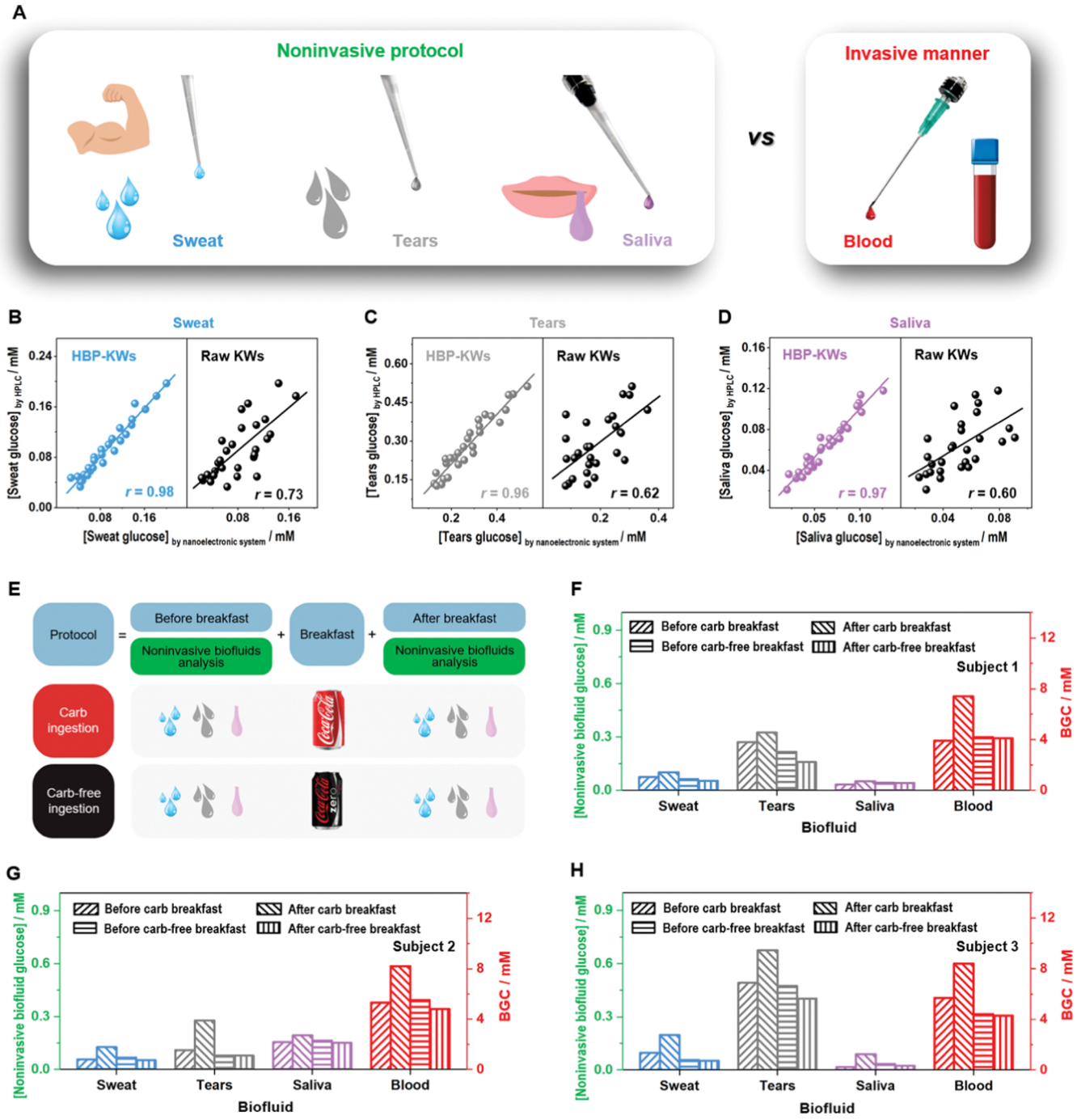

Figure 4. Validation of the universal fully integrated nanoelectronic system for point-of-care raw noninvasive biofluid glucose monitoring of sweat, tears, or saliva. (A) Schematics of raw noninvasive biofluid (sweat, tears, and saliva) glucose monitoring versus raw invasive biofluid (blood) glucose monitoring. (B–D) Validation of the universal fully integrated nanoelectronic system with the HBP-KWs (left) or raw KWs (right) microchannel for raw sweat, tears, or saliva glucose measurement using HPLC analysis. Each type of noninvasive biofluids is collected from four subjects (Subject 1–4). (E) Schematics of the protocols to investigate the effect of carbohydrate food intake on noninvasive biofluid (sweat, tears, and saliva) glucose in controlled environments. (F–H) Dependence of the sweat, tears, saliva, or blood glucose level before breakfast and 1 h after breakfast from three healthy subjects (Subject 1–3) upon carbohydrate or carbohydrate-free food ingestion.

only different types of noninvasive biofluids but also the same types of noninvasive biofluids from the same subject obtained at different times always exhibit different pH values[41] and ionic strengths.[42−46] Thus, besides the wide linear range and exceptional selectivity, another critical challenge to fulfill the accurate glucose analysis in various raw noninvasive biofluids by one universal biosensor is its capability to suppress biofluids' physiological pH and ionic strength effects on i*ez*Slice's response. To tackle such a challenge, an HBP-KWs microchannel was particularly constructed and incorporated into the i*ez*Slice. Benefiting from the forced constant/same pH and high ionic strength nature of the HBP on the fluids, the i*ez*Slice with the HBP-KWs microchannel exhibits outstanding physiological pH- and ionic strength-independent response stabilities on the artificial biofluids of raw sweat, tears, or saliva with a defined volume of 0.30 μL in comparison to the

https://doi.org/10.1021/acs.analchem.1c05174
Anal. Chem. 2022, 94, 1890−1900

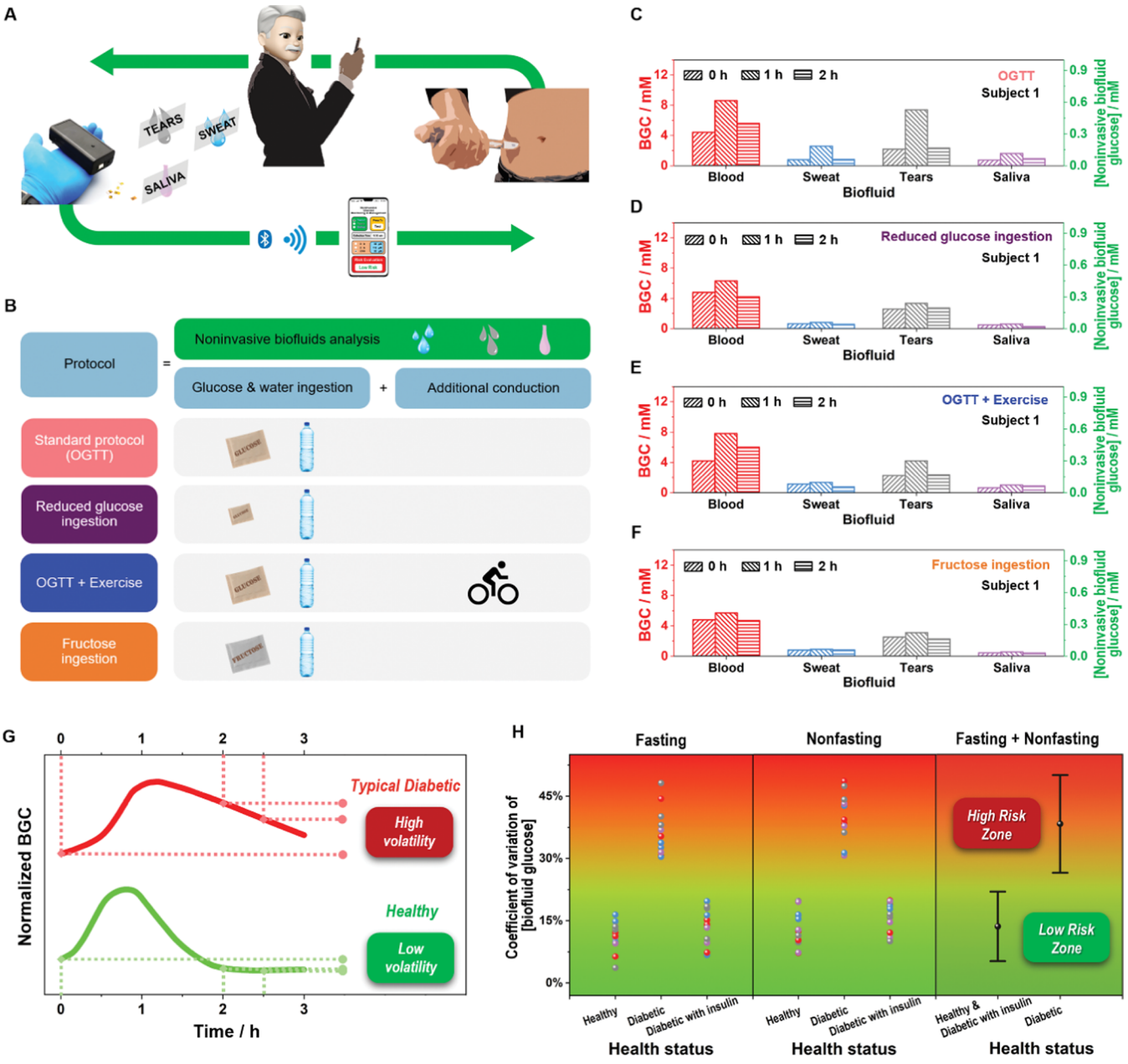

Figure 5. Utilization of the universal fully integrated nanoelectronic system for potential noninvasive glucose management. (A) Schematic illustration of the universal fully integrated nanoelectronic system for potential noninvasive glucose management by utilizing sweat, tears, or saliva glucose as the biomarker. (B) Schematics of certain scenarios simulating real situations that are related to human BGC variation in controlled environments. (C–F) Dependence of the sweat, tears, saliva, or blood glucose level upon OGTT times of 0, 1, and 2 h with different protocols mentioned in (B). (G) Schematics of the comparison of the volatility of BGCs between the typical diabetic and healthy subjects before and after the carbohydrate intake with the carbohydrate intake time at 0 h. (H) Dependence of the coefficients of variation on the biofluid (red, light blue, light dark, and purple balls represent the blood, sweat, tears, and saliva, respectively) glucose levels of healthy, diabetic, and insulin-treated diabetic subjects (Subject 1–6) at OGTT times of 0, 2 and 2.5 h with fasting (left) or nonfasting (middle) states, which are derived from Figures S14–S19 and Tables S19 and S20. Statistical analysis of the coefficients of variation on the biofluid glucose levels of healthy and insulin-treated diabetic subjects and diabetic subjects with both fasting and nonfasting states (right), which are derived from the left and middle figures of (H). Error bars represent the two standard deviations that stand for a 95% confidence interval.[36,37]

unsatisfied performance at the *iez*Slice with the raw Kimwipes (KWs) or low-concentration-buffer powder-loaded KWs (LBP-KWs) microchannel (Figures S10 and S11). Such impressive capacity highlights a critical role of the HBP treatment in ensuring high accuracy for glucose analysis in different types of noninvasive raw biofluids of sweat, tears, and saliva with a wide physiological pH range from 4 to 8[41] and a wide physiological ionic strength range from 10 mM Na^+, 2 mM K^+, and 0.2 mM Ca^{2+} to 165 mM Na^+, 42 mM K^+ and 6.2 mM Ca^{2+},[42−46] respectively.

By combining the wide dynamic range, exceptional specificity, and outstanding physiological pH-/ionic strength-independent response stabilities with high mechanical (Figure 2K–M) and storage stabilities (Table S12) and acceptable reproducibility (Table S13), the remarkable analytical performance of the *iez*Slice may make it extremely promising for the

https://doi.org/10.1021/acs.analchem.1c05174
Anal. Chem. 2022, 94, 1890−1900

direct raw sweat, tears, or saliva glucose analysis without any pretreatment.

Design and Performance Characterization of *iez*Slice Microfluidics. Because of its inherent features of the small volume of samples, fast sampling, and ready miniaturization, microfluidics has been extensively utilized as a full or integrative unit of point-of-care diagnostic electronic devices.[47,48] However, traditional microfluidics requires an external cumbersome pumping system to maintain the regular operation, which may greatly weaken devices' practicability.[49] To avoid such a case, we fabricated a single piece of HBP-KWs as the pump-free microchannel of the *iez*Slice (Figure 3A,B). As revealed by the numerical simulations (Figure 3C,D), the filling time of sweat taken to reach 100% of the new solute concentration was as fast as ∼0.73 s for the solute concentration changing from 0 to 60 μM within single-piece HBP-KWs by setting the experimentally obtained sweat flow rate (0.665 μL s^{-1}, Supporting Information) as the inlet flow rate. During the on-microchip testing, driven by the capillarity, the single-piece HBP-KWs microchannel spontaneously and effectively gathered raw human sweat from an unpumped pipette tip with a high temporal resolution, matching pretty well with those indicated by the numerical simulations demonstrated above (Figure 3D,E). In addition, it was proved that a sweat volume down to 0.30 μL is sufficient to completely fill the HBP-KWs microchannel (Table S14). These attractive peculiarities make the HBP-KWs microchannel highly promising for effective and efficient noninvasive biofluid (e.g., sweat, tears, or saliva) sampling and further glucose analysis.

Validation of the Fully Integrated Nanoelectronic System with Point-of-Care Raw Sweat, Tears, or Saliva Glucose Monitoring. Noninvasive biofluids (e.g., sweat, tears, and saliva) contain a variety of biochemicals that can be indicative of underlying physiological conditions and bring promising new applications for healthcare (Figure 4A).[15] Recent research studies reported several interesting fully integrated biosensors for raw sweat,[14] tears,[30] or saliva[31] glucose measurement. However, none of them can act as a universal one to meet the glucose analysis in all three typical raw noninvasive biofluids of sweat, tears, and saliva till now. By connecting a flexible and disposable *iez*Slice with a reusable and wireless *iez*Bar, we assembled the universal fully integrated nanoelectronic system and determined its accuracy for the direct glucose analysis in raw sweat, tears, or saliva samples using high-performance liquid chromatography (HPLC), and each kind of biofluids was collected from four subjects (Tables S15−S18). In comparison to a relatively low Pearson's correlation coefficient (r, ≤0.73) at the universal fully integrated nanoelectronic system with the raw KWs microchannel (Figure 4B−D), the universal fully integrated nanoelectronic system with the HBP-KWs microchannel exhibits a much higher r value (≥0.96) for raw sweat, tears, or saliva glucose analysis, which suggests a key role of the HBP-KWs microchannel within the universal fully integrated nanoelectronic system in the highly accurate and reliable raw noninvasive biofluid measurement.

In consideration that the glucose concentration variations in the noninvasive biofluids of sweat, tears, and saliva may be related to carbohydrate food intake,[11,14,21−27,30,31] we conducted controlled food ingestion trials on healthy subjects to validate the universal fully integrated nanoelectronic system for point-of-care raw noninvasive biofluid glucose monitoring (Figure 4E). As expected, an obvious enhancement in sweat, tears, or saliva glucose was observed following the carbohydrate food (classic Coca-Cola, 600 mL) intake in comparison to no increased response with the carbohydrate-free one (Coca-Cola Zero, 600 mL), which is similar to the trend of blood glucose (Figure 4F−H). In addition, it was observed that the glucose levels in noninvasive biofluids (i.e., sweat, tears, and saliva in this work) were individual-dependent. Subject 1's sweat glucose concentrations before and after carbohydrate breakfast, for example, are higher than the corresponding ones in saliva, which contrasts with Subject 2's scenario (Figure 4F,G). Such a phenomenon is likely attributable to the personalized variations among individuals.[22]

Utilization of the Universal Fully Integrated Nanoelectronic System for Potential Noninvasive Glucose Management. Glucose management is crucial for both healthy and diabetic individuals since keeping the blood glucose concentration (BGC) as close to the target range as much as possible helps prevent/delay long-term or major health problems and is also beneficial for enhancing people's energy and mood.[50] Compared to the traditional invasive blood glucose analysis, the noninvasive manner without piercing human skin exhibits the distinctive features of nearly no risk of injury or infection and high-degree user-friendliness (Figure 5A).[15,51]

We set the oral glucose tolerance test (OGTT) that is currently the "gold standard" for diagnosing diabetes mellitus in clinical practice[52] as the standard protocol and carried out controlled trials that could affect the BGC (Figure 5B): (a) The dose of glucose ingestion: For a recruited healthy subject during the OGTT, the fasting BGC measured by a commercial kit started at 4.4 mM before the glucose solution intake, reached 8.6 mM at 1 h, and returned to a lower level of <7 mM at 2 h (Figure 5C), indicating the subject body's normal ability to metabolize glucose.[52] By reducing glucose ingestion, the BGC at 1 h decreased accordingly (Figure 5D), which could be due to lower-dose glucose ingestion inducing less glucose in human biofluids. Meanwhile, the noninvasive biofluid (raw sweat, tears, and saliva) glucose variations were recorded and their trends showed high agreement with those of the BGCs (Figure 5D). (b) Exercise: With the implementation of exercise during the OGTT, the BGC at 1 h substantially reduced to 7.8 mM compared to the routine OGTT (Figure 5E), which would be attributed to the increased skeletal muscle glucose consumption during the exercise.[53] Such an obvious downward trend has been synchronously illustrated by noninvasive biofluid glucose (Figure 5E). (c) The type of sugar: In comparison to the standard protocol of the OGTT with glucose ingestion, the intake of fructose resulted in a lower glucose level at 1 h (Figure 5F), signifying fructose's lower capacity to increase BGC, which could be attributed to the metabolic mechanisms of fructose. Fructose can be converted to glucose in the body: however, fructose is predominantly converted into glucose or triglyceride by the liver in normal humans and most of the formed glucose is stored as glycogen, which results in a modest increase in the BGC.[54] The studies mentioned above demonstrate a similar trend in BGC and the noninvasive biofluid glucose level before and after glucose intake in different control experiments (Figures 5B−F, S12, and S13), which suggests a possibility to achieve noninvasive glucose management with the universal fully integrated nanoelectronic system.

https://doi.org/10.1021/acs.analchem.1c05174
Anal. Chem. 2022, 94, 1890−1900

The conventional manner to achieve noninvasive biofluid-derived noninvasive glucose management relies on the glucose level correlation between the noninvasive biofluids and the blood.[1−3,5,9,10] Recent progress highlights the vital role of the personalized correlations in individual noninvasive glucose management with improved accuracy,[22] which suggests the possibly required one-to-one personalized precorrelation for each individual's routine noninvasive glucose management that may accordingly increase extra workload. Considering that a more significant fluctuation feature of the typical diabetic ones' BGCs before and after carbohydrate ingestion could be found compared to the healthy ones' because the diabetic subjects lose part of or the whole BGC regulation function,[55] we introduced the volatility concept that is frequently used for data dispersibility evaluation in the descriptive statistics[56] into noninvasive glucose management (Figure 5G). The preliminary study indicated that by collecting/analyzing the biofluid (blood, sweat, tears, or saliva) glucose at times of 0, 2, and 2.5 h through either or both the conventional fasting OGTT (i.e., a clinical standard manner for diabetes mellitus diagnosis) and the nonfasting OGTT (mimicking daily meal), a significant statistical difference was found between the "low risk" subjects whose BGCs were assumed to be well regulated naturally or artificially (e.g., healthy and insulin-treated diabetic subjects) and the "high risk" ones whose BGCs were assumed to be not well regulated naturally or artificially (e.g., diabetic subjects; Supporting Information, Figures 5H and S14−S19, and Tables S19 and S20). These demonstrate the feasibility of such a volatility-derived BGC-free protocol to make a risk assessment on hyperglycemia and also signify a promising and convenient way to realize noninvasive biofluid glucose management due to its inherent and exceptional BGC-free trait. In light of the fact that sweat and tears were both collected by external stimulation (i.e., iontophoresis technique for sweat and tears stick for tears) in the current work but saliva does not need external stimulation, so saliva could be more convenient, suitable, and attractive for diabetes management. Considering the limited number of subjects participating in the current investigation, future work may involve the integration of big data[57] and machine learning[58] to achieve highly precise noninvasive glucose management.

CONCLUSIONS

In summary, this work successfully illustrated the first instance of a universal fully integrated nanoelectronic system that is composed of an *iez*Slice (i.e., a specially designed flexible, pump-free, and single-use microfluidic enzymatic biosensor) and an *iez*Bar (i.e., a custom, wireless, handheld, and reusable potentiostat), which enables a highly accurate point-of-care glucose analysis in various types of raw noninvasive biofluids (sweat, tears, and saliva) for potential noninvasive glucose management without any component replacement within the system or raw sample pretreatment. As a point-of-care testing device, the present universal fully integrated nanoelectronic system exhibits a sequence of exceptional features: (1) The introduction of HBP-KWs into the universal fully integrated nanoelectronic system as the microchannel of the *iez*Slice allows the unique universal glucose analysis of three types of common raw noninvasive biofluids (sweat, tears, and saliva) but without accuracy compromise, which would readily deal with the unexpected problems that single-type biofluid glucose analysis cannot resolve (for example, sweat, tears, and saliva glucose analysis could be inapplicable for subjects with dermatosis, oculopathy, hematuria, and psychosis, respectively). (2) The utilization of 3D-CNAs with the distinctive three-dimensional carbonaceous nanoscale network architecture as the electrode material of the *iez*Slice allows a wide enough glucose detection linear range that fully covers the physiological glucose levels of all three types of raw human noninvasive biofluids (i.e., sweat, tears, and saliva) and accordingly guarantees the universal noninvasive biofluid glucose analysis. (3) The ultralow volume of 0.30 μL required for the noninvasive biofluid analysis by the universal fully integrated nanoelectronic system enables the very quick sample collection, which may facilitate high time resolution monitoring of the noninvasive biofluid biomarkers. On the other hand, the direct examination of such ultralow raw noninvasive biofluids encourages potential timely noninvasive glucose management and control without causing skin prick, thus enhancing the self-monitoring compliance of the subjects. (4) The fully integrated configuration notion-guided design achieves the distinctive complete functional implementation of the universal fully integrated nanoelectronic system with point-of-care noninvasive biofluid glucose monitoring, signifying much higher practicality compared to the commonly reported unintegrated ones focusing on limited components, such as only microfluidic parts or solo enzymatic electrodes. (5) Glucose management is important, especially challenging for diabetes mellitus because diabetic patients have to frequently monitor their BGCs to assess the effectiveness of the personalized medical treatment and make a timely adjustment to the treatment if the BGC is not within the target range. To evaluate the utility of the universal fully integrated nanoelectronic system as a clinical and physiological investigation tool for potential noninvasive glucose management, we employed the volatility concept and applied our BGC-free solution to conduct a preliminary study toward noninvasive glucose management, illustrating its most enticing and convenient feature. Future work may entail big data and machine learning to improve the proposed statistical model for precise noninvasive glucose management in different and complex situations. (6) The substitution of the GOx enzyme within the *iez*Slice by different biomimetic receptors may readily achieve diverse biomarker monitoring in raw noninvasive biofluids, indicating the high versatility of the universal fully integrated nanoelectronic system for a wide range of personalized diagnostic and physiological monitoring applications. The combination of these distinctive and appealing aspects with an ultralow feedstock cost of ∼USD 0.02 per *iez*Slice (test) makes such a universal fully integrated nanoelectronic system based on the flexible microfluidic chip surpass the preponderance and practicability of conventional noninvasive biofluid glucose biosensors or recently reported fully integrated raw noninvasive biofluid glucose biosensors and have a wide spectrum of application prospects in the low-cost point-of-care raw noninvasive biofluid analysis for potential noninvasive glucose management. Though several unique advantages were demonstrated above, the current universal fully integrated nanoelectronic system requires a specific volume of raw samples (0.30 μL) to guarantee the accurate measurement, implying that the sample volume-free devices could be the more attractive and advanced ones that are being attempted with substantial efforts for noninvasive biofluid analysis in both industry and academia.

https://doi.org/10.1021/acs.analchem.1c05174
Anal. Chem. 2022, 94, 1890−1900

■ ASSOCIATED CONTENT

Supporting Information

The Supporting Information is available free of charge at https://pubs.acs.org/doi/10.1021/acs.analchem.1c05174.

Materials and reagents; characterization and measurements; construction of the iezSlice; characterization of the 3D-CNAs; electrocatalysis of glucose at the 3D-CNA- and CNT-based iezSlices; storage stability and reproducibility of the iezSlice; effects of physiological pH and physiological Na^+, K^+, and Ca^{2+} concentrations in artificial noninvasive biofluids on the iezSlice response; COMSOL simulations on single-piece HBP-KWs microfluidics; filling volume determination; and validation/utilization for point-of-care raw noninvasive biofluid glucose monitoring and potential noninvasive glucose management (PDF)

■ AUTHOR INFORMATION

Corresponding Author

Ming Zhou − *Key Laboratory of Polyoxometalate and Reticular Material Chemistry of Ministry of Education, National & Local United Engineering Laboratory for Power Batteries, Key Laboratory of Nanobiosensing and Nanobioanalysis at Universities of Jilin Province, Analysis and Testing Center, Department of Chemistry, Northeast Normal University, Changchun, Jilin Province 130024, China*; orcid.org/0000-0003-2239-9342; Email: zhoum739@nenu.edu.cn

Authors

Mimi Sun − *Key Laboratory of Polyoxometalate and Reticular Material Chemistry of Ministry of Education, National & Local United Engineering Laboratory for Power Batteries, Key Laboratory of Nanobiosensing and Nanobioanalysis at Universities of Jilin Province, Analysis and Testing Center, Department of Chemistry, Northeast Normal University, Changchun, Jilin Province 130024, China*

Xinyi Pei − *Key Laboratory of Polyoxometalate and Reticular Material Chemistry of Ministry of Education, National & Local United Engineering Laboratory for Power Batteries, Key Laboratory of Nanobiosensing and Nanobioanalysis at Universities of Jilin Province, Analysis and Testing Center, Department of Chemistry, Northeast Normal University, Changchun, Jilin Province 130024, China*

Tong Xin − *Key Laboratory of Polyoxometalate and Reticular Material Chemistry of Ministry of Education, National & Local United Engineering Laboratory for Power Batteries, Key Laboratory of Nanobiosensing and Nanobioanalysis at Universities of Jilin Province, Analysis and Testing Center, Department of Chemistry, Northeast Normal University, Changchun, Jilin Province 130024, China*

Jian Liu − *Key Laboratory of Polyoxometalate and Reticular Material Chemistry of Ministry of Education, National & Local United Engineering Laboratory for Power Batteries, Key Laboratory of Nanobiosensing and Nanobioanalysis at Universities of Jilin Province, Analysis and Testing Center, Department of Chemistry, Northeast Normal University, Changchun, Jilin Province 130024, China*

Chongbo Ma − *Key Laboratory of Polyoxometalate and Reticular Material Chemistry of Ministry of Education, National & Local United Engineering Laboratory for Power Batteries, Key Laboratory of Nanobiosensing and Nanobioanalysis at Universities of Jilin Province, Analysis and Testing Center, Department of Chemistry, Northeast Normal University, Changchun, Jilin Province 130024, China*

Mengzhu Cao − *Key Laboratory of Polyoxometalate and Reticular Material Chemistry of Ministry of Education, National & Local United Engineering Laboratory for Power Batteries, Key Laboratory of Nanobiosensing and Nanobioanalysis at Universities of Jilin Province, Analysis and Testing Center, Department of Chemistry, Northeast Normal University, Changchun, Jilin Province 130024, China*

Complete contact information is available at: https://pubs.acs.org/10.1021/acs.analchem.1c05174

Author Contributions

The manuscript was written through contributions of all authors. All authors have given approval to the final version of the manuscript.

Notes

The authors declare no competing financial interest.

■ ACKNOWLEDGMENTS

The authors acknowledge the support from the "111" Project (China, No. B18012), the Fundamental Research Funds for the Central Universities (China, Nos. JGPY201802, 2412020ZD006, and 2412019QD008), the Jilin Provincial Department of Education (China), the Key Laboratory of Nanobiosensing and Nanobioanalysis at Universities of Jilin Province (China), and Analysis and Testing Center of Northeast Normal University (China).

■ REFERENCES

(1) Zhao, J.; Guo, H.; Li, J.; Bandodkar, A. J.; Rogers, J. A. *Trends Chem.* **2019**, *1*, 559−571.

(2) Lin, Y.; Bariya, M.; Javey, A. *Adv. Funct. Mater.* **2021**, *31*, No. 2170290.

(3) Wang, M.; Yang, Y.; Gao, W. *Trends Chem.* **2021**, *3*, 969−981.

(4) Wang, L.; Chen, J.; Wang, J.; Li, H.; Chen, C.; Feng, J.; Guo, Y.; Yu, H.; Sun, X.; Peng, H. *Sci. China Chem.* **2021**, *64*, 1763−1769.

(5) He, X.; Yang, S.; Liu, C.; Xu, T.; Zhang, X. *Adv. Healthcare Mater.* **2020**, *9*, No. 2000941.

(6) Liu, Z.; Tian, Y. *Sci. China Chem.* **2021**, *64*, 915−931.

(7) Jiang, X.; Wang, Q.; Wang, Z.; Dong, B.; Huang, L.; Chi, L. *Chem. Res. Chin. Univ.* **2021**, *37*, 975−988.

(8) Li, D.; Wu, C.; Tang, X.; Zhang, Y.; Wang, T. *Chem. Res. Chin. Univ.* **2021**, *37*, 803−822.

(9) Lee, H.; Hong, Y. J.; Baik, S.; Hyeon, T.; Kim, D.-H. *Adv. Healthcare Mater.* **2018**, *7*, No. 1701150.

(10) Mohan, A. M. V.; Rajendran, V.; Mishra, R. K.; Jayaraman, M. *TrAC, Trends Anal. Chem.* **2020**, *131*, No. 116024.

(11) Emaminejad, S.; Gao, W.; Wu, E.; Davies, Z. A.; Yin Yin Nyein, H.; Challa, S.; Ryan, S. P.; Fahad, H. M.; Chen, K.; Shahpar, Z.; Talebi, S.; Milla, C.; Javey, A.; Davis, R. W. *Proc. Natl. Acad. Sci. U.S.A.* **2017**, *114*, 4625.

(12) van den Akker, R.; van den Hoek, J. A.; van den Akker, W. M.; Kooy, H.; Vijge, E.; Roosendaal, G.; Coutinho, R. A.; van Loon, A. M. *AIDS* **1992**, *6*, 953−957.

(13) Lifshitz, M.; Weinstein, O.; Gavrilov, V.; Rosenthal, G.; Lifshitz, T. *Ther. Drug Monit.* **1999**, *21*, 544−546.

(14) Gao, W.; Emaminejad, S.; Nyein, H. Y. Y.; Challa, S.; Chen, K.; Peck, A.; Fahad, H. M.; Ota, H.; Shiraki, H.; Kiriya, D.; Lien, D. H.; Brooks, G. A.; Davis, R. W.; Javey, A. *Nature* **2016**, *529*, 509−514.

(15) Kim, J.; Campbell, A. S.; de Ávila, B. E.-F.; Wang, J. *Nat. Biotechnol.* **2019**, *37*, 389−406.

(16) Steil, G. M.; Panteleon, A. E.; Rebrin, K. *Adv. Drug Delivery Rev.* **2004**, *56*, 125−144.
(17) Rowley, W. R.; Bezold, C.; Arikan, Y.; Byrne, E.; Krohe, S. *Popul. Health Manage.* **2017**, *20*, 6−12.
(18) Lee, H.; Choi, T. K.; Lee, Y. B.; Cho, H. R.; Ghaffari, R.; Wang, L.; Choi, H. J.; Chung, T. D.; Lu, N.; Hyeon, T.; Choi, S. H.; Kim, D.-H. *Nat. Nanotechnol.* **2016**, *11*, 566−572.
(19) Jin, X.; Li, G.; Xu, T.; Su, L.; Yan, D.; Zhang, X. *Biosens. Bioelectron.* **2022**, *196*, No. 113760.
(20) Teymourian, H.; Barfidokht, A.; Wang, J. *Chem. Soc. Rev.* **2020**, *49*, 7671−7709.
(21) Sempionatto, J. R.; Lin, M.; Yin, L.; De la paz, E.; Pei, K.; Sonsa-ard, T.; de Loyola Silva, A. N.; Khorshed, A. A.; Zhang, F.; Tostado, N.; Xu, S.; Wang, J. *Nat. Biomed. Eng.* **2021**, *5*, 737−748.
(22) Sempionatto, J. R.; Moon, J.-M.; Wang, J. *ACS Sens.* **2021**, *6*, 1875−1883.
(23) Yu, Y.; Nassar, J.; Xu, C.; Min, J.; Yang, Y.; Dai, A.; Doshi, R.; Huang, A.; Song, Y.; Gehlhar, R.; Ames Aaron, D.; Gao, W. *Sci. Robot.* **2020**, *5*, No. eaaz7946.
(24) Lee, H.; Song, C.; Hong, Y. S.; Kim, M. S.; Cho, H. R.; Kang, T.; Shin, K.; Choi, S. H.; Hyeon, T.; Kim, D.-H. *Sci. Adv.* **2017**, *3*, No. e1601314.
(25) He, X.; Fan, C.; Xu, T.; Zhang, X. *Nano Lett.* **2021**, *21*, 8880−8887.
(26) Song, Y.; Min, J.; Yu, Y.; Wang, H.; Yang, Y.; Zhang, H.; Gao, W. *Sci. Adv.* **2020**, *6*, No. eaay9842.
(27) De la Paz, E.; Barfidokht, A.; Rios, S.; Brown, C.; Chao, E.; Wang, J. *Anal. Chem.* **2021**, *93*, 12767−12775.
(28) Karpova, E. V.; Shcherbacheva, E. V.; Galushin, A. A.; Vokhmyanina, D. V.; Karyakina, E. E.; Karyakin, A. A. *Anal. Chem.* **2019**, *91*, 3778−3783.
(29) Martín, A.; Kim, J.; Kurniawan, J. F.; Sempionatto, J. R.; Moreto, J. R.; Tang, G.; Campbell, A. S.; Shin, A.; Lee, M. Y.; Liu, X.; Wang, J. *ACS Sens.* **2017**, *2*, 1860−1868.
(30) Sempionatto, J. R.; Brazaca, L. C.; García-Carmona, L.; Bolat, G.; Campbell, A. S.; Martin, A.; Tang, G.; Shah, R.; Mishra, R. K.; Kim, J.; Zucolotto, V.; Escarpa, A.; Wang, J. *Biosens. Bioelectron.* **2019**, *137*, 161−170.
(31) Arakawa, T.; Tomoto, K.; Nitta, H.; Toma, K.; Takeuchi, S.; Sekita, T.; Minakuchi, S.; Mitsubayashi, K. *Anal. Chem.* **2020**, *92*, 12201−12207.
(32) Chen, W.; Zhang, X.; Mi, L.; Liu, C.; Zhang, J.; Cui, S.; Feng, X.; Cao, Y.; Shen, C. *Adv. Mater.* **2019**, *31*, No. 1806664.
(33) Li, Z.; Wu, D.; Huang, X.; Ma, J.; Liu, H.; Liang, Y.; Fu, R.; Matyjaszewski, K. *Energy Environ. Sci.* **2014**, *7*, 3006−3012.
(34) Banks, C. E.; Davies, T. J.; Wildgoose, G. G.; Compton, R. G. *Chem. Commun.* **2005**, *10*, 829−841.
(35) Banks, C. E.; Moore, R. R.; Davies, T. J.; Compton, R. G. *Chem. Commun.* **2004**, 1804−1805.
(36) Sen, D. K.; Sarin, G. S. *Br. J. Ophthalmol.* **1980**, *64*, No. 693.
(37) Dickinson, E. J. F.; Limon-Petersen, J. G.; Rees, N. V.; Compton, R. G. *J. Phys. Chem. C* **2009**, *113*, 11157−11171.
(38) Tsierkezos, N. G.; Ritter, U. *Phys. Chem. Liq.* **2012**, *50*, 661−668.
(39) Wan, K.; Yu, Z.-p.; Li, X.-h.; Liu, M.-y.; Yang, G.; Piao, J.-h.; Liang, Z.-x. *ACS Catal.* **2015**, *5*, 4325−4332.
(40) Doretti, L.; Ferrara, D.; Gattolin, P.; Lora, S. *Talanta* **1997**, *44*, 859−866.
(41) Corrie, S. R.; Coffey, J. W.; Islam, J.; Markey, K. A.; Kendall, M. A. F. *Analyst* **2015**, *140*, 4350−4364.
(42) Baker, L. B.; Wolfe, A. S. *Eur. J. Appl. Physiol.* **2020**, *120*, 719−752.
(43) Farandos, N. M.; Yetisen, A. K.; Monteiro, M. J.; Lowe, C. R.; Yun, S. H. *Adv. Healthcare Mater.* **2015**, *4*, 792−810.
(44) Sarigul, N.; Korkmaz, F.; Kurultak, İ. *Sci. Rep.* **2019**, *9*, No. 20159.
(45) Foley, K. F.; Boccuzzi, L. *Lab. Med.* **2010**, *41*, 683−686.
(46) Pytko-Polonczyk, J. J.; Jakubik, A.; Przeklasa-Bierowiec, A.; Muszynska, B. *J. Physiol. Pharmacol.* **2017**, *68*, 807−813.
(47) Gervais, L.; de Rooij, N.; Delamarche, E. *Adv. Mater.* **2011**, *23*, H151−H176.
(48) Akceoglu, G. A.; Saylan, Y.; Inci, F. *Adv. Mater. Technol.* **2021**, *6*, No. 2100049.
(49) Nge, P. N.; Rogers, C. I.; Woolley, A. T. *Chem. Rev.* **2013**, *113*, 2550−2583.
(50) Penckofer, S.; Quinn, L.; Byrn, M.; Ferrans, C.; Miller, M.; Strange, P. *Diabetes Technol. Ther.* **2012**, *14*, 303−310.
(51) He, X.; Yang, S.; Pei, Q.; Song, Y.; Liu, C.; Xu, T.; Zhang, X. *ACS Sens.* **2020**, *5*, 1548−1554.
(52) American Diabetes Association. *Diabetes Care* **2018**, *41*, S13−S27.
(53) Kjøbsted, R.; Roll, J. L. W.; Jorgensen, N. O.; Birk, J. B.; Foretz, M.; Viollet, B.; Chadt, A.; Al-Hasani, H.; Wojtaszewski, J. F. P. *Diabetes* **2019**, *68*, 1427−1440.
(54) Crapo, P. A.; Kolterman, O. G.; Olefsky, J. M. *Diabetes Care* **1980**, *3*, 575−582.
(55) Raffel, L. J.; Goodarzi, M. O. Diabetes Mellitus. In *Reference Module in Biomedical Sciences*; Elsevier, 2014.
(56) Holcomb, Z. *Fundamentals of Descriptive Statistics*, 1st ed.; Routledge, 2016.
(57) Shilo, S.; Rossman, H.; Segal, E. *Nat. Med.* **2020**, *26*, 29−38.
(58) Mateen, B. A.; Liley, J.; Denniston, A. K.; Holmes, C. C.; Vollmer, S. J. *Nat. Mach. Intell.* **2020**, *2*, 554−556.

https://doi.org/10.1021/acs.analchem.1c05174
Anal. Chem. 2022, 94, 1890−1900